Full-Wave Analysis of A Line-Fed Rectangular Patch Antenna Using FDTD Method with Mur's and PML ABCs

التحليل الشامل للهوائى المستطيل والمغذى بواسطة الخط الشريطى الدقيق باستخدام طريقة الفروق المحدودة فى الحيز الزمنى مع كل من شروط الامتصاص الحدية لمير والطبقات المتوائمة تماما

Maher M. Abd Elrazzak, ***IEEE Member*****, A. N. Mahmoud, and**
H. Elmikati, ***IEEE Senior Member***
Facluty of Eng., Mansoura Univ., El-Mansoura, Egypt.
email: maher@ieee.org

Key-words:- FDTD, Mur's, PML, and Patch Antenna

فى هذا البحث تم استخدام طريقة الفروق المحدودة فى الحيز الزمنى (FDTD) لتحليـــل الـــهوائى الشريطـــى المســتطيل والمغذى بواسطة الخط الشريطى الدقيق مع استحدام كل من الطبقات المتوائمة تماما لبرينجر (Berenger's PML) وكذلك شـــروط الامتصاص الحدية لمير ذات الدرجة الأولـــى(Mur's FOC) . ولـــهذا الـــهوائـــى تـــم حســاب المجـــال فـــى الحـــيز الزمنـــى (Time domain field response) و الفقد الناتج عن الانعكاس (return loss) والمعاوقة الداخلية (input impedance). و كذلك تم دراسة تأثير عرض الهوائى (width) ومكان تغذيتة (feeder displacement) على خصائصه.

وقد وجد أن النتائج التى تم الحصول عليها بطريقة الفروق المحدودة فى الحيز الزمنى باستخدام الطبقات تامة المواءمة أكثر تقاربا مع النتائج المعملية المنشورة عن مثيلاتها التى تم الحصول عليها بطريقة الفروق المحدودة مع اسخدام شروط الامتصاص الحديـــة لمير ذات الدرجة الأولى.

Abstract- In this paper, the finite-difference time-domain (FDTD) method is used for the analysis of a line-fed rectangular patch antenna. This is carried out by using the Berenger perfectly matched layer (PML) as well as Mur's first order absorbing boundary conditions (Mur's FOC). The time domain field response, the return loss, and the input impedance of the structure are obtained. In addition, the effect of patch width and the feeder displacement are studied. The results obtained by the FDTD with PML are found to be in better agreement with the published measured data than those obtained by the FDTD with Mur's FOC .

I-Introduction

The finite-difference time-domain (FDTD) technique is one of the most popular Maxwell's equations solution techniques [1-3]. This technique was initially formulated by Yee [1]. It has been widely applied to various electromagnetic problems such as scattering problems [1,4], modeling of microstrip and CPW structures [5-6], and antenna analysis [7-8].

The main advantages of FDTD technique are, simplicity, ability to handle complex structures, and to obtain the response over a wide frequency band from one calculation. FDTD approach is a direct solution of Maxwell's time dependent curl equations. The basic idea of this method is based upon volumetric sampling of unknown field distribution (E and H) within and

Accepted June 27, 1999

surrounding the structure of interest, and over a period of time. The sampling in space and time is selected to give the desired accuracy and the numerical stability of the algorithm, respectively. FDTD method is a marching in time procedure that simulates the continuos actual propagation of electromagnetic waves in a specific region. Time stepping continues until the desired late-time pulse response is observed at the field points of interest. At these points, a wide band frequency response can be obtained by Fourier transformation of the transient response. Since the simulation of the electromagnetic waves in open structures requires that the modeled region must extend to infinity, absorbing boundary conditions (ABCs) are employed at certain outer grid truncation planes. to eliminate the reflections from the outgoing waves to the computational domain. These ABCs include, for example, Mur's ABCs [9], and Berenger perfectly matched layer (PML) [10-11] which are used in the present work.

The main theme of this paper is to use the FDTD method to obtain the time domain response, the return loss, and the input impedance of a microstrip patch antenna. The method is based upon employing both Mur's FOC, and perfectly matched absorber. In the next sections, a brief outline of FDTD method, Mur's FOC, and PML ABCs are presented. Next, the analysis of a line-fed rectangular patch antenna with its numerical results and concluding remarks are given.

II. Formulation of the problem

II.A Basic FDTD principles

This section presents the basic formulation of FDTD method. The actual dimensions of the microstrip patch antenna are shown in Fig. 1, where the strips and the bottom plane are perfect conductors with zero thickness. The substrate has a dielectric constant ε_r.

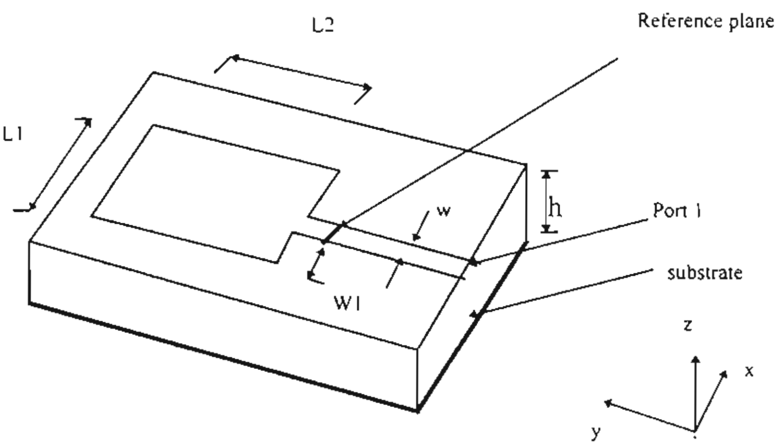

Fig. 1. Line-fed rectangular patch antenna

For this structure, Maxwell's equations can be written as[1],

$$\frac{\partial \bar{H}}{\partial t} = -\frac{1}{\mu}\nabla x \bar{E} - \frac{\rho'}{\mu}\bar{H} \tag{1.1}$$

$$\frac{\partial \bar{E}}{\partial t} = \frac{1}{\varepsilon}\nabla x \bar{H} - \frac{\sigma}{\varepsilon}\bar{E} \tag{1.2}$$

where,

ρ' is the magnetic resisitivity of the medium in (Ω/m)

σ is the electric conductivity of the medium in (S/m)

$\frac{\partial}{\partial t}[\bullet]$ is the partial derivative with respect to time

Equations (1) are approximated using the second order central difference scheme in space and time [1-3]. The orientation of the electric and magnetic field components in a unit cell of FDTD lattice is shown in Fig.2. The position of E-and H-nodes are off in space by $\Delta/2$ space. The difference equations of the six field components in Cartesian coordinate of equation (1) are given, for instance, in references[2] and [3]. For example, the discretized equations for H_x and E_x field components are,

$$H_x\Big|_{i,j,k}^{n+1/2} = D_a\Big|_{i,j,k} \cdot H_x\Big|_{i,j,k}^{n-1/2} + D_b\Big|_{i,j,k}\left\{\frac{E_y\Big|_{i,j,k+1/2}^{n} - E_y\Big|_{i,j,k-1/2}^{n}}{\Delta z} - \frac{E_z\Big|_{i,j+1/2,k}^{n} - E_z\Big|_{i,j-1/2,k}^{n}}{\Delta y}\right\} \tag{2.1}$$

$$E_x\Big|_{i,j,k}^{n+1} = C_a\Big|_{i,j,k} \cdot E_x\Big|_{i,j,k}^{n} + C_b\Big|_{i,j,k}\left\{\frac{H_z\Big|_{i,j+1/2,k}^{n+1/2} - H_z\Big|_{i,j-1/2,k}^{n+1/2}}{\Delta y} - \frac{H_y\Big|_{i,j,k+1/2}^{n+1/2} - H_y\Big|_{i,j,k-1/2}^{n+1/2}}{\Delta z}\right\} \tag{2.2}$$

where Δx, Δy, and Δz are the space steps in the x, y, and z directions respectively, the D's, and the C's are the updating electric and magnetic field components coefficients, respectively [2].

To ensure that the numerical error generated in one step does not accumulate and grow, the stability condition is applied according to Courant relation given by [2-3],

$$\Delta t \le \frac{1}{v_{max}}\left(\frac{1}{\Delta x^2} + \frac{1}{\Delta y^2} + \frac{1}{\Delta z^2}\right)^{-\frac{1}{2}} \quad)$$

where

Δt is the maximum time step that may be used,

v_{max} is the velocity of light in the computational domain

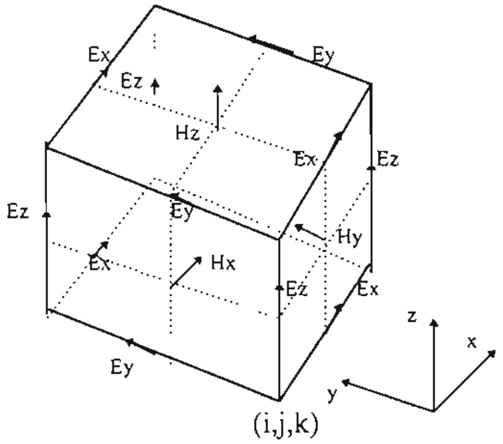

Fig.2. The orientation of the electric and magnetic field components in Yee's FDTD cell

II.B Mur's first order ABC

Mur's first order ABC is characterized by its simplicity for implementation. In this approach the one-way wave equation may be written as [9].

$$\left(\partial z - c^{-1}\partial t\right)W\big|_{y=0} = 0 \tag{4.1}$$

where,

W denote to the tangential electric field components.

c denote to the velocity of light

It is assumed that the mesh is located in the region $y\geq 0$ as shown in Fig.1 and the excited pulse will be normal to the mesh walls. The boundary conditions for plane y=o,(front wall) are expressed in terms of the tangential electric field components E_x and E_z .The finite -difference formulation of equation(4.1) can be written as [9],

$$E_o^{n+1} = E_1^n + \frac{c\Delta t - \Delta z}{c\Delta t + \Delta z}\left(E_1^{n+1} - E_o^n\right) \tag{4.2}$$

where,

E_o is the electric field components E_x or E_z on the front wall

E_1 is the electric field components E_x or E_z on the first node inside the front wall

In a similar manner. one can write the other tangential electric field components at the other mesh walls.

II.C- PML-ABC

The PML technique consists in surrounding the computational domain of an open structure with an artificial lossy medium whose impedance is matched to free space for all frequencies and all incident angles [10-11]. The ability to absorb the outgoing waves is provided by the additional degrees of freedom introduced by splitting the field components within the anisotropic material properties [10-11]. With the splitting of the field components, the six Maxwell's field equations are replaced by twelve equations. For instance, the H_x and E_x field equations are written as [10-11].

$$\mu_o \frac{\partial H_{xy}}{\partial t} + \sigma_y^* H_{xy} = -\frac{\partial (E_{zx} + E_{zy})}{\partial y} \tag{5. a}$$

$$\mu_o \frac{\partial H_{xz}}{\partial t} + \sigma_z^* H_{xz} = \frac{\partial (E_{yx} + E_{yz})}{\partial z} \tag{5. b}$$

$$\varepsilon_o \frac{\partial E_{xy}}{\partial t} + \sigma_y E_{xy} = \frac{\partial (H_{zx} + H_{zy})}{\partial y} \tag{6. a}$$

$$\varepsilon_o \frac{\partial E_{xz}}{\partial t} + \sigma_z E_{xz} = -\frac{\partial (H_{yx} + H_{yz})}{\partial z} \tag{6. b}$$

where,

σ^* denotes the magnetic loss.

The reflectionless condition of the PML medium is given by

$$\frac{\sigma}{\varepsilon_o} = \frac{\sigma^*}{\mu_o} \tag{7}$$

This relationship ensures that the wave impedance inside the PML is equal to the free-space wave impedance, and that the phase velocity inside the PML is the vacuum speed of light. To ensure that there is no any reflections from PML regions to the computational domain, the amplitude of the wave propagating inside the PML is exponentially attenuated and absorbed. This is carried out by forcing the losses in the PML medium to increase gradually with the depth d_e of the PML layers. Thus the electric loss is set to zero at the interface between the FDTD domain and PML inner boundary (interface between the PML and the FDTD domain). The dependence of the loss on the depth can be assumed of the form

$$\sigma_i(d_e) = \sigma_{max}\left(\frac{d_e}{\delta}\right)^n \tag{8}$$

where,

δ denotes the PML thickness,

σ_i denotes either σ_x, σ_y or σ_z,

n is an exponent which indicates the rate of increase of loss with depth,

d_e denotes the depth of the PML medium, and

σ_{max} denotes the maximum electric conductivity.

The magnetic losses is assumed to vary within the PML medium in the same manner as the electric loss.

To update the field components within the PML medium, the updated coefficients of the electric and magnetic field components given by the standard Yee's algorithm can not be used. This is due to the fact that the attenuation of the propagating waves within the PML medium is so rapid. Therefore these coefficients are replaced by exponentially decaying coefficients within the PML medium [2].

III. Analysis of a line-fed rectangular patch antenna

The analyzed patch antenna is shown in Fig.1. The space steps used are Δx =0.389mm, Δy =0.400mm, and Δz =0.265 mm. The total mesh dimensions are 60x100x16 in the x, y, and z directions, respectively. The rectangular patch antenna has $L1=32\Delta x$, and $L2=40\Delta y$. The length of the microstrip line from the source plane to the edge of the antenna is $50\Delta y$. The reference plane is $10\Delta y$ from the edge of the patch. The width of microstrip line w is $6\Delta x$, the displacement w1 is $5\Delta x$, the substrate thickness h is $3\Delta z$, and $13\Delta z$ are used to model the free space above the substrate. The substrate dielectric constant is 2.2.

In the present analysis, a Gaussian pulse with unit amplitude is excited on the microstrip line at the edge of the computation domain i.e. at port 1 (source plane) as shown in Fig.1. This pulse is given by:

$$E_z(t) = e^{-\frac{(t-t_o)^2}{T^2}} \tag{9}$$

where,

$\Delta t = 0.441$ ps,

T: Gaussian half width = 15 ps,

$t_o = 3T$

Initially all the fields on the whole computation domain are set to zero. After the pulse has propagated away port 1, absorbing boundary conditions are implemented several cells from the source. The transient response are recorded at the reference plane until all the fields in the computation domain decay to a negligible steady-state value. Then the Fourier transformation is used to obtain the return loss, and the input impedance of the patch antenna according to [5].

Fig. 3. shows the field distribution of the electric field components E_x, E_y, and E_z at the plane, $y=40\Delta y$, $z=10\Delta z$, and $200\Delta t$ time steps. The results have been obtained using FDTD with mixed boundary conditions of Mur's FOC and PML absorber . In this figure, LR denotes that all absorbing walls are taken as Mur's FOC except the left and right walls which are carried out as PML absorber, while FB only uses PML in the front and back walls and the other walls are Mur's FOC. The thickness of the PML absorber is taken as 8 cells.

To determine the reflection coefficient of the patch, one must calculate the refelected wave at the reference plane. This is carried out by two FDTD simulations. The first simulation is for the analyzed structure which gives the refelected and incident waves (total) at the reference plane. The second simulation is for a nonreflecting structure with the identical input (i.e the feeder extended to ABC). This provides a pure incident wave at the reference plane. Then the reflected wave is computed as the difference between the total (output of the first simulation) and the incident waveform(output of the second simulation).

Figs. 4 and 5 show the transient time response of the E_z component at the reference plane for both uniform microstrip line's feeder and patch antenna, respectively.

The transient time response of E_z field component just underneath the dielectric-air interface at 200, 400, 600, 800,1000 and 1200 Δt time steps are shown in Fig.6 where the excitation pulse and subsequent propagation on the antenna are observed.

From incident and reflected waves, one can calculate the return loss and then the input impedance of the proposed structure using Fourier transformations. Fig.7 shows the return loss of the patch antenna up to 20 GHz. The results have been obtained using FDTD with Mur's FOC or PML for all absorber walls. Comparing the obtained results with the measured data in [5], it is found that the PML results are in better agreement with the measured data than those obtained by either the Mur's FOC or LR. in particular for determining the locations of the resonance frequencies.

The real and imaginary parts of the input impedance of this antenna up to 20 GHz are shown in Fig.8 and Fig. 9, respectively. From these figures, it can be seen that at resonance frequencies the input impedance is pure real, especially for the case of using FDTD with PML absorber.

Focusing on the effect of patch width (L1) variation on the characteristics of the present patch antenna, it is found that the resonance frequencies as well as the return loss are increased with decreasing L1 as shown in Fig.10. In addition, both the real and imaginary parts of the input impedance increase as shown in Figs11 and 12. respectively. The data in the last figures are obtained by FDTD with PML absorber.

Fig.13. shows the effect of feeder displacement (w1) on the return loss of the patch antenna. From this figure, one can observe that the return loss is inversely proportional with the displacement due to the mismatch losses at the interface between the feeder and the patch, while the resonance frequency locations remain at the same values[12].

The input impedance corresponding to each of the cases studied in Fig. 13, is shown in Figs. 14 and 15.

IV. Conclusion.

In this paper. the finite- difference time- domain FDTD method with the Breneger perfect matched layer. and Mur's FOC has been used to determine the time domain response. the return loss. and the input impedance of a line- fed rectangular patch antenna . This technique is characterized by its simplicity. ability to handle complex structures, and wide frequency response from one calculation. The effect of patch width and feeder displacement are studied. The results obtained by the FDTD with perfect matched layer absorber are found to be in much better agreement with the published measured data than those obtained by the FDTD with Mur's FOC.

REFERENCES

[1] K. S. Yee. " Numerical solution of initial boundary value problems involving Maxwell's equations in isotropic media," IEEE Trans. Antennas Propagat.," vol. AP-14. pp.302- 307; May.1966.

[2] Allen Taflove. Computational Electrodynamics:The Finite-Difference Time- Domain Method. Artech House, Boston. London.1995.

[3] Karl. S. Kuenz and Raymound J. Luebbers. The Finite- Difference Time-Domain Method for Electromagnetics. CRC press. London- Tokyo, 1993.

[4] C. M. Furse. S. P. Mathur. and O. Gandhi." Improvements to finite-difference time-domain method for calculating the radar cross section of perfectly conducting target." IEEE Trans., Microwave Theory Tech. vol. MTT-38. No.7. pp. 919-927. July. 1990.

[5] D. M. Sheen. S. M. Ali. M. D. Abouzahra. and J. A.Kong. "Application of the three-dimensional finite-difference time-domain method to the analysis of planar microstrip circuits." IEEE Trans.. Microwave Theory Tech. vol. MTT-38. No.7. pp. 849-857. July. 1990.

[6] Huan-Shang Tsai, and Robert A. York. "FDTD analysis of CPW-fed folded-slot and multiple-slot antennas on thin substrates." IEEE Trans. Antennas Propagat.,vol.44. No.2. pp.217- 226, Feb.1996.

[7] Candid Reig, Enrique A. Navarro, and Vicente Such, " F D T D analysis of E- sectoral horn antennas for broad-band applications. IEEE Trans. Antennas Propagat.,vol.45. No.10. pp.1484-1487, Oct.1997.

[8] S. Shum. and K. Luck, "FDTD analysis of probe-fed cylindrical dielectric resonator antenna," IEEE Trans. Antennas Propagat.,vol.46. No.3. pp.325- 333, Mar.1998.

[9] Mur G.. " Absorbing boundary conditions for the finite-difference approximation of the time-domain." Electromagnetic Compatt., vol. 23, No. 4, pp. 377 - 382, Nov.1981.

[10] Jean - Pierre Berenger. " A perfectly matched layers for the FDTD solution of wave-structure interaction problems," IEEE.Trans. Antennas Propagat.,vol.44, No. 1, pp.110-117, Jan. 1996.

[11] R. Mittra, and U. Pekel, "A new look at the perfectly matched layer (PML)concept for the reflectionless absorption of electromagnetic waves," IEEE Microwave and Guided Wave lett. vol.5. No.3, pp.84-86. Mar.1995.

[12] C. A. Balanis, Antenna Theory: Analysis and Design, New York, John Wiley & Sons Inc. 1997.

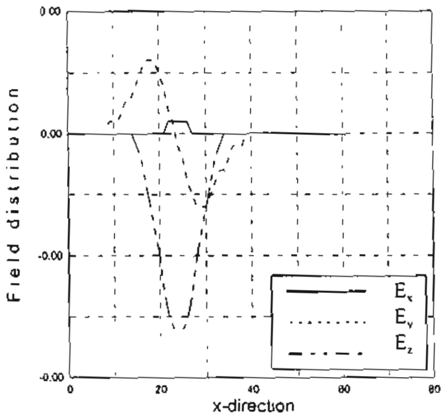

(a)Mur's FOC for all walls

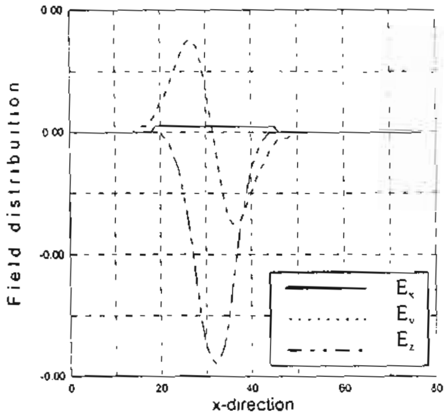

(b)Mur's FOC with PML at side walls

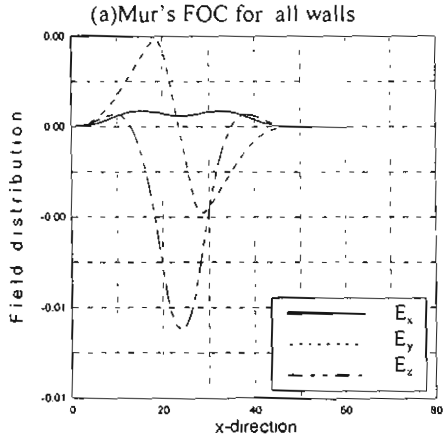

(c) Mur's FOC with PML at front and back walls

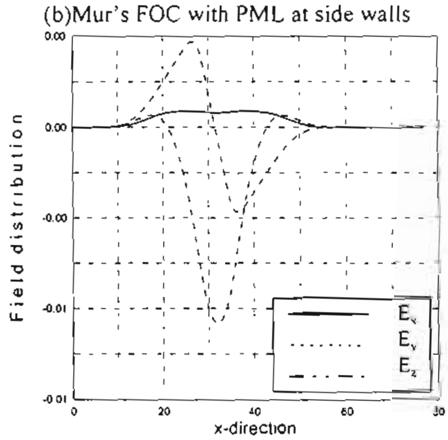

(d) PML for all walls

Fig. 3. The field distribution versus the substrate width at $y=40\Delta y$, $z=10\Delta z$, and $t=200\Delta t$

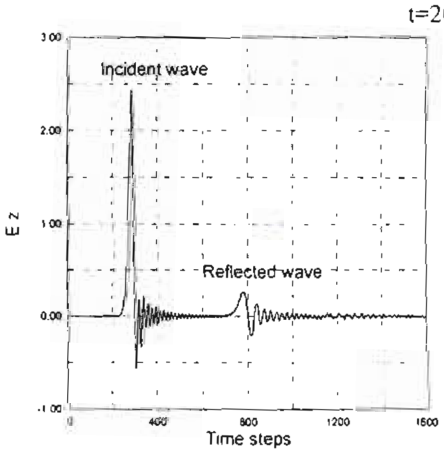

Fig. 4. The incident and reflected waves at reference plane on a uniform microstrip line

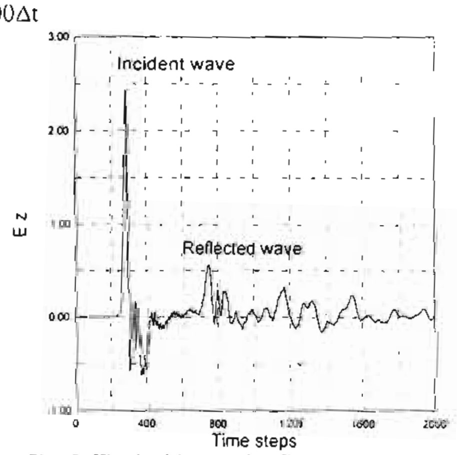

Fig. 5. The incident and reflected waves at reference plane on patch microstrip antenna

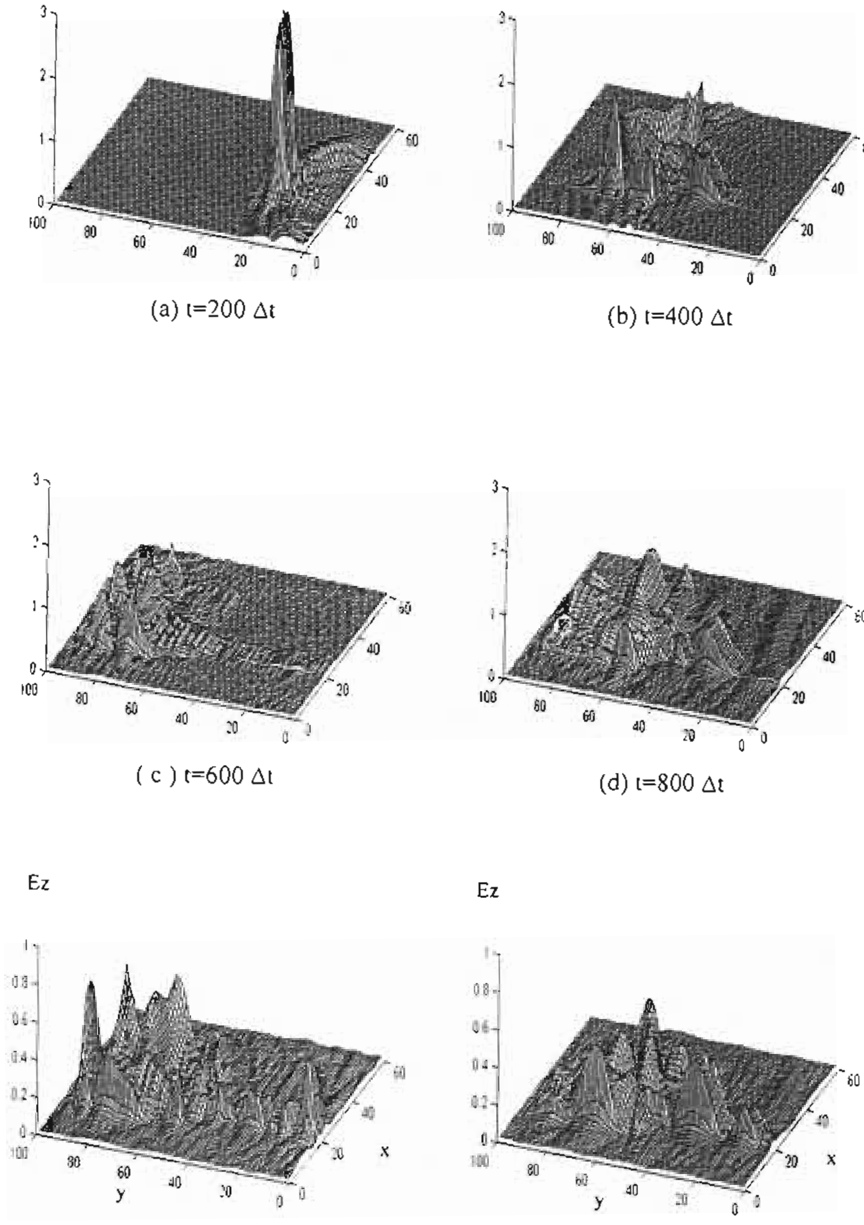

(a) t=200 Δt

(b) t=400 Δt

(c) t=600 Δt

(d) t=800 Δt

(e) t=1000 Δt

(f) t=1200 Δt

Fig. 6. Time-domain field response of the rectangular patch antenna

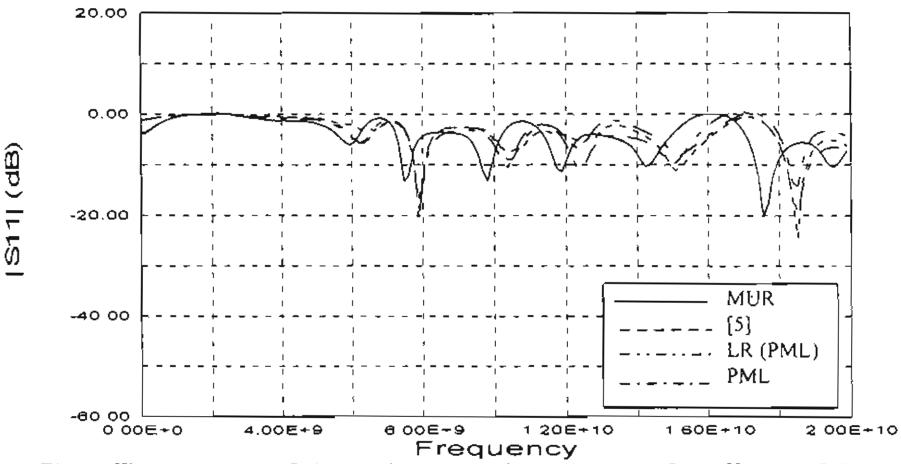

Fig. 7. The return loss of the patch antenna shown in Fig. 1 for different ABCs

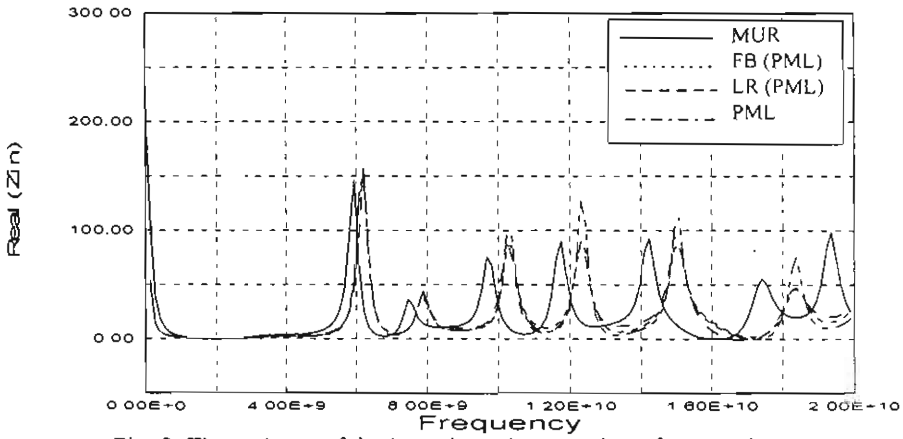

Fig. 8. The real part of the input impedance at the reference plane of the patch antenna shown in Fig. 1

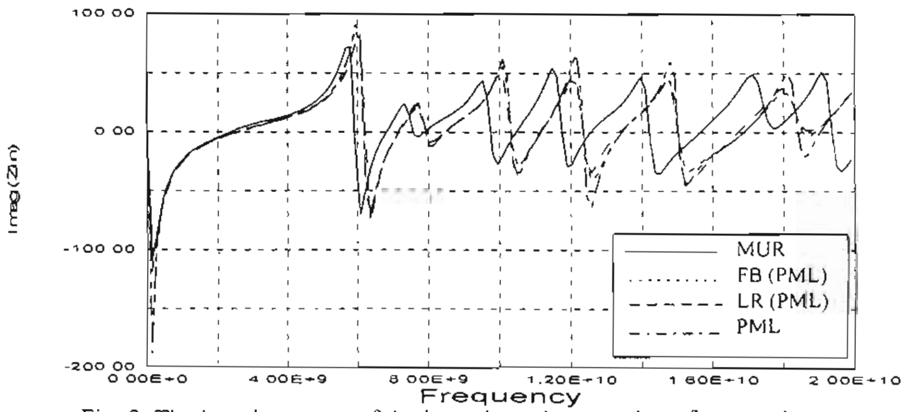

Fig. 9. The imaginary part of the input impedance at the reference plane of the patch antenna shown in Fig. 1